Planning Shortest Bounded–Curvature Paths for a Class of Nonholonomic Vehicles among Obstacles

Antonio Bicchi* Giuseppe Casalino Corrado Santilli
Centro "E. Piaggio" & Dipartimento Sistemi Elettrici e Automazione
Università di Pisa

Abstract

This paper describes a technique for path planning in environments cluttered with obstacles for mobile robots with nonholonomic kinematics and bounded trajectory curvature (i.e., limited turning radius). The method is inspired by the results of Reeds and Shepp regarding shortest paths of bounded curvature in absence of obstacles. It is proved that, under suitable assumptions, the proposed technique provides the shortest path of bounded curvature among polygonal objects for a particular class of vehicles (circular unicycles of radius h and minimum turning radius $\rho_{min} \leq h$). Although the class of vehicles this theoretical result is restricted to is rather narrow, the proposed planner can be satisfactorily applied to other nonholonomic vehicles yielding good practical results.

1 Introduction

Motion planning for nonholonomic vehicles is attracting a wide interest in Robotics.

A nonholonomic constraint is an equation involving the configuration parameters and their derivatives (velocity parameters) that is not integrable. Such constraints do not reduce the dimension of the robot configuration space (like holonomic constraints do), but reduce the dimension of the velocity space at any given configuration. A fundamental result of nonlinear system theory shows that nonholonomic systems, notwithstanding the reduced number of inputs, remain completely controllable if the degree of nonholonomy is sufficient ([9]). Barraquand and Latombe [2] proved that a car–like robot with curvature limitations moving amidst obstacles remains fully controllable, that is, whenever a free (holonomic) trajectory exists, the existence of a feasible path is also guaranteed.

The presence of lower bounds on the minimum turning radius involves curvature constraints on feasible trajectories that deeply affect the geometry of the problem. Dubins [6] and Reeds and Shepp [12] solved the geodesic problem without and with reversals, respectively, and showed that a path with shortest length can always be built by concatenating at most five linear or circular segments. Similar results have been elegantly derived again by Sussmann and Tang [13] and Boissonnat, Cerezo, and Leblond [3], using Pontryagin's maximum principle. These theoretical results ignited a new series of methods tending to find shortest nonholonomic paths with bounded curvature amidst obstacles, among which [7], [8], [11].

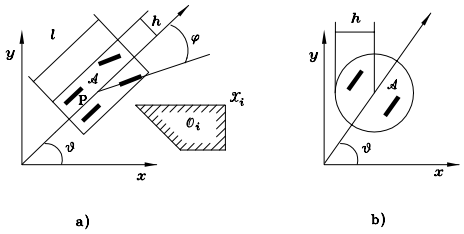

Figure 1: A generic car–like robot (a) and a particular unicycle vehicle (b).

The method presented in this paper is also inspired by Reeds and Shepp's work, in that the resulting path is a simple concatenation of linear and circular segments of maximum curvature. The main theoretical result proved in this paper concerns shortest paths of a particular vehicle (a circular unicycle of radius h and minimum turning radius $\rho_{min} \leq h$) moving among polygonal obstacles. Theorem 1 states that, if the proposed planner succeeds in finding a path, and if that path is regular (i.e., without reversals), then that is a shortest feasible path of bounded curvature for the given problem. The principal worth of the proposed method is perhaps in its simplicity and in the smoothness of the resulting paths. It does not require explicit evaluation of the configuration space, nor it employs a preliminary phase of holonomic trajectory planning. The method can be applied to both unicycle and car–like mobile robots of general shape, provided that some simple heuristics are introduced to overcome most typical deadlocks for

*Corresponding author, bicchi@vm.cnuce.cnr.it

the planner. Simulation and experimental results are reported demonstrating the viability of the method in medium–complexity environments.

2 Problem and Proposed Solution

Fig.1–a shows a mobile robot, modelled as a two dimensional object $\mathcal{A}$ moving in a 2–dimensional workspace.

The configuration space of the robot is $\mathbb{R}^2 \times S^1$, and can be locally parameterized by the coordinates x and y of the robot reference point P, and by the angle θ (representing the robot orientation) between the x–axis of the base frame $\mathcal{F}_\mathcal{S}$ and the main axis of the robot. The robot shape is assumed symmetric with respect to its main axis, and its half-width is denoted by h. We restrict ourselves to consider only polygonal obstacles in the workspace, that we indicate with $\mathcal{O}_i$, $i = 1, \ldots, l$, while their n vertices are listed in $\mathcal{X}_j$, for $j = 0$ to n. A nonholonomic constraint arises because the wheels can roll and spin but not slip, hence the robot cannot move sidewise. For a unicycle vehicle such as that shown in fig.1–b, the nonholonomic constraint is written as

$$S(\mathbf{q})\dot{\mathbf{q}} = \begin{bmatrix} -\sin(\theta) & \cos(\theta) & 0 \end{bmatrix} \begin{bmatrix} \dot{x} \\ \dot{y} \\ \dot{\theta} \end{bmatrix} = 0$$

The motion planning problem can be stated as follows:

Problem 1 *Let $\mathbf{q}_s = (x_s, y_s, \theta_s)$ and $\mathbf{q}_g = (x_g, y_g, \theta_g)$ be respectively the initial and final configuration of a robot $\mathcal{A}$ with minimum turning radius ρ_{min} and half-width h. Determine a path $\bar{\mathbf{q}}(\tau)$ that minimizes the cost functional*

$$J(\bar{\mathbf{q}}(\cdot)) \stackrel{def}{=} \int_0^T \sqrt{x'^2(\tau) + y'^2(\tau)}\, d\tau, \qquad (1)$$

subject to

$$\bar{\mathbf{q}}(0) = \mathbf{q}_s; \qquad (2)$$

$$\bar{\mathbf{q}}(1) = \mathbf{q}_g; \qquad (3)$$

$$\mathcal{A}(\bar{\mathbf{q}}(\tau)) \cap \mathcal{O}_i = \emptyset \;\; i = 1, \ldots, l, \;\; \forall \tau \in [0, 1]; \qquad (4)$$

$$S(\bar{\mathbf{q}})\bar{\mathbf{q}}' = 0, \;\; \forall \tau \in [0, 1]; \qquad (5)$$

$$\bar{\mathbf{q}}(\tau) \in C^1, \text{ and } \frac{x'y'' - x''y'}{(x'^2 + y'^2)^{3/2}} \leq \frac{1}{\rho_{min}}, \qquad (6)$$

where $\bar{\mathbf{q}}' = \frac{d\bar{\mathbf{q}}(\tau)}{d\tau}$, $x' = \frac{dx(\tau)}{d\tau}$, $y' = \frac{dy(\tau)}{d\tau}$, $x'' = \frac{d^2x(\tau)}{d\tau^2}$, $y'' = \frac{d^2y(\tau)}{d\tau^2}$.

Finding a solution to this problem is quite difficult in general. However, previous results on shortest paths of bounded curvature in free environments can be extended to give a qualitative description of the solution of Problem 1, when considering the particular class of mobile robot with circular shape of radius h, and minimum turning radius $\rho_{min} = h$ (see fig.1–b)

Proposition 1 *The solution (if one exists) of Problem 1 for circular vehicles with $\rho_{min} = h$ is a concatenation of line segments and arcs of circle of radius ρ_{min}.*

Proof. Problem 1 can be cast in the standard optimal programming form by rewriting (5) in explicit form as

$$\begin{aligned} \dot{x} &= v\cos\theta \\ \dot{y} &= v\sin\theta \\ \dot{\theta} &= \omega \end{aligned} \qquad (7)$$

or, in compact form, as $\dot{\mathbf{q}} = f(\mathbf{q}, \mathbf{u})$. The curvature constraint (6) is translated in bounds on the input vector $\mathbf{u} = (v, \omega) \in U \subset \mathbb{R}^2$, where $U = \{-1, +1\} \times \{-1/\rho_{min}, 1/\rho_{min}\}$. It is also possible to rewrite holonomic constraints due to the presence of obstacles, (4), in the form of a set of m inequality constraints on functions of the states of the system as

$$K_i(\mathbf{q}) \leq 0, \quad i = 1, \ldots, m$$

According to the treatment of optimal control in bounded phase space given by Chang [4], introduce the variational Hamiltonian

$$\mathcal{H}(\mathbf{q}, \mathbf{u}, \lambda, \eta) = J(\mathbf{q}, \mathbf{u}) + \eta^T \mathbf{K}(\mathbf{q}) + \lambda^T f(\mathbf{q}, \mathbf{u})$$

where

$$\eta_i \begin{cases} = 0, & K_i(\mathbf{q}) < 0 \\ \neq 0, & K_i(\mathbf{q}) = 0 \end{cases}$$

Correspondingly, the optimal trajectory will be composed of free and constrained arcs. Along constrained arcs ($K_i(\mathbf{q}) = 0$) the robot is in touch with an obstacle. Due to the geometry of the robot and of the obstacles, constrained arcs are composed of line segments (the robot is "grazing" an edge) and of circular arcs of radius h (the robot is turning about a vertex).

To evaluate optimal trajectories along free arcs ($K_i(\mathbf{q}) < 0, \forall i$), it is expedient to reformulate the minimization problem by defining a new variable $z(t)$ as

$$\dot{z} = \sqrt{\dot{x}^2 + \dot{y}^2}, \quad z(0) = 0.$$

The corresponding Hamiltonian can be written as

$$\bar{\mathcal{H}}(\bar{\mathbf{q}}, u, \bar{\lambda}_f) = < \bar{\lambda}_f, \dot{\bar{\mathbf{q}}} > = w\dot{z} + pv\cos\theta + qv\sin\theta + k\omega$$

where $\bar{\mathbf{q}} = (z, \mathbf{q})$, and $\bar{\lambda} = (w, p, q, k)$. Application of Pontryagin's maximum principle to this system with the input bounds above described leads to distinguish

between unconstrained arcs along which i) $\frac{\partial \mathcal{H}}{\partial \omega} \equiv 0$, or ii) $\frac{\partial \mathcal{H}}{\partial \omega} \neq 0$. Full discussion of these cases is reported by Boissonnat, Cerezo, and Leblond [3], and shows that either the arc is a line segment (case i), or an arc of a circle of radius ρ_{min}. □

Note that existence of a solution to problem 1 is not always guaranteed, as shown by Desaulniers [5]. This is not in contrast with the minimum principle, which only gives necessary conditions.

Motivated by the above qualitative result on optimal trajectories, we introduce the following algorithm, which is described with reference to a generic vehicle:

Algorithm 1

a) *Draw n circles with radius $\rho = \max\{\rho_{min}, h\}$ centered in the obstacle vertices. Also draw two circles with radius ρ_{min} passing through $[x_s,\ y_s]$ and tangent to the line through $[x_s,\ y_s]$ with angle θ_s, and an analogous pair of circles for the final configuration $\mathbf{q}_g$.*

b) *Consider the $n+4$ circles two at a time, and draw the four linear segments belonging to the common tangent lines and comprised between the tangency points. Also consider all arcs on circles that join any two tangency points. Let a basic path diagram (BPD) be composed of two directed segments for each of these linear and circular segments.*

c) *The BPD may contain non–free paths, that is, paths that cannot be followed by the robot without colliding with obstacles. Directed segments are then tested singularly and those causing collisions are eliminated from the diagram. In general, a segment may be free if followed in one sense, but not otherwise. For robots that are simmetric with respect to a line through the reference point and normal to the main axis of the robot, the direction of motion along a path is not relevant, and a simpler basic path diagram can be considered.*

d) *A directed graph G is built from the thus emended path diagram (EPD) as follows:*

- *the start and goal configurations are nodes of G;*
- *for all points of tangency between a linear and a circular segment, two configurations (corresponding to the possible orientations aligned with the common tangent direction) are nodes of G;*
- *two nodes i and j of G are connected with an oriented link from i to j if the corresponding directed segment on the emended path diagram exists;*
- *a cost equal to the length of the corresponding segment is associated to each link.*

e) *The directed graph G is searched for a path from the start to the goal configuration using the length of the overall path as the cost function.*

The following theorem discusses a property of the planner algorithm when applied to the special class of circular robots above considered:

Theorem 1 *For a circular mobile robot $\mathcal{A}$ with radius h equal to the minimum turning radius ρ_{min} moving in a bidimensional polygonal workspace $\mathcal{S}$, a sufficient condition for a path to be the solution of problem 1 is that it is a regular output of the proposed planner.*

Proof. Consider the problem (Problem 2) of finding the shortest element in the class of paths composed of line segments and circular arcs of radius ρ_{min} and avoiding the obstacles in the given workspace. A characteristic of paths in this class is that their first (last) arc or segment belong to one of the two circles of radius ρ_{min} tangent in the start (goal) to the initial (final) direction, or on the line through the start (goal) with the initial (final) direction.

Path(s) solving Problem 2 are shorter than, or equal to, paths solving Problem 1. This follows trivially from Proposition 1. Note that solutions to Problem 2 may fail to meet the condition on the correct orientation of the vehicle at the goal configuration.

It will now be proved that the path provided by the planner algorithm 1, whenever is regular (without cusps), coincides with the solution of Problem 2. In fact, the EPD corresponds to a generalized visibility diagram built taking into consideration the original obstacles grown by ρ_{min} and the two pairs of circles tangent in the start and in the goal to the initial and final direction. Shortest paths on a generalized visibility diagram are proved to be shortest feasible paths and to be always regular (see e.g. Latombe [10]). The thesis then follows from observing that the shortest path on the EPD, if regular, coincides with the shortest path on the visibility diagram and therefore is the solution of Problem 2. □

3 Discussion

Although of some relevance to the as yet unexplored problem of global optimal path planning amidst obstacles, Theorem 1 only provides sufficient results for a particular vehicle. In this section we list some of the pitfalls of the proposed method along with simple heuristics that may help in applying the planner to more realistic robots.

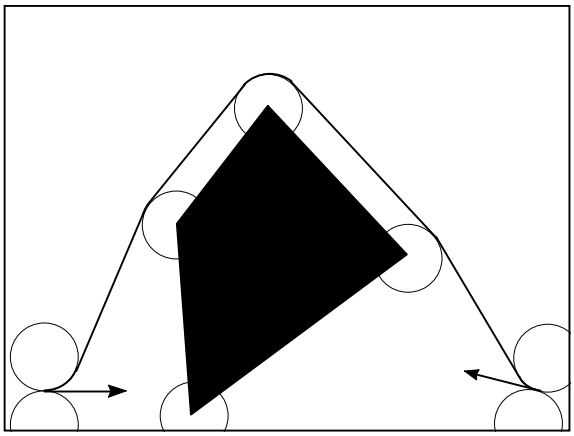

Figure 2: Impossibility to maneuver with too few obstacles.

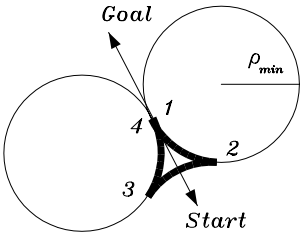

Figure 3: A Reeds/Shepp inversion pattern (a) can be introduced to solve the deadlock of fig 2 (b).

Remark 1. Only sufficiency results have been established because of two main reasons. Firstly, if the planner results in a path that contains reversals, visibility graph arguments can not be applied in the proof. Piecewise optimality of paths between reversals can still be argued, but global path optimality remains unsolved.

Secondly, the method is not path–complete. For the circular robot of concern in theorem 1, incompleteness may be caused by the impossibility to maneuver without the support of an obstacle vertex. Consider for instance the case depicted in fig. 2, where the robot can use neither any of the obstacle circles to make the necessary reversal, nor the start and goal pairs of circles because of space limitations. A simple heuristic solution to this problem is to find a cell in free space where a Reeds/Shepp inversion pattern (see fig. 3) can be accomodated for, and to consider the corresponding additional pair of circles in the algorithm. In building the Reeds/Shepp inversion pattern, existing circles are

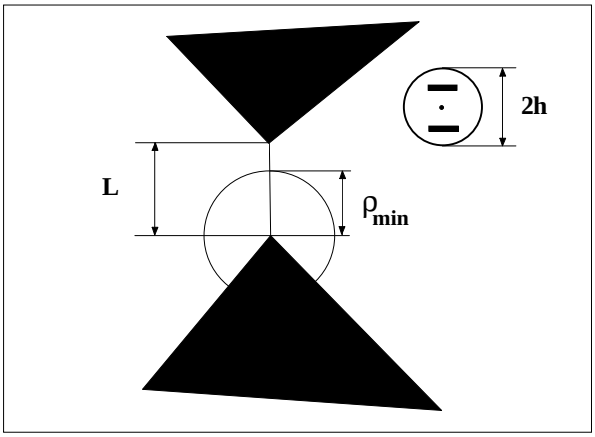

Figure 4: A possible deadlock for the algorithm

considered first, as this usually requires less clearance. Notice that introduction of auxiliary circles produces a graph G' that includes the original graph G, hence the search on G' provides a path whose length is at least equal to the shortest path on G.

In fact, a characteristic of the proposed planner is its suitability to highly cluttered environments, where it accomplishes its best performance. The method's weaknesses are more evident when the scarceness of obstacles does not offer support to enough circles and, therefore, maneuver possibilities. An instance of such a problem is put into evidence by the parallel parking problem. In fact, the proposed algorithm can park a circular robot of radius R if the clearance is larger than three times R, while from the above mentioned controllability results we know that parking is theoretically possible in slots just larger than $2R$. There is probably no easy fix to this problem, as its solution is only possible by approximating a non–feasible trajectory with a very high number of nonholonomic maneuvers (this is actually what the method of Jacobs *et al.* [8] does in this case).

Remark 2. If $\rho_{min} \neq h$, the circular segments of BPD are drawn with radius $\rho = \max\{\rho_{min}, h\}$. If $\rho_{min} < h$, the algorithm is applied similarly, except for circles at the start and goal, that are drawn with radius ρ_{min}. The optimality properties of algorithm 1 are still retained in this case. Also Reeds/Shepp inversion patterns can be introduced, if necessary, using circles of radius ρ_{min}.

If $\rho_{min} > h$, path–completeness of the method is further reduced in cases such as that depicted in fig. 4, where the vertex–to–vertex distance L is such that $2 * h < L < h + \rho_{min}$. An heuristic fix to this prob-

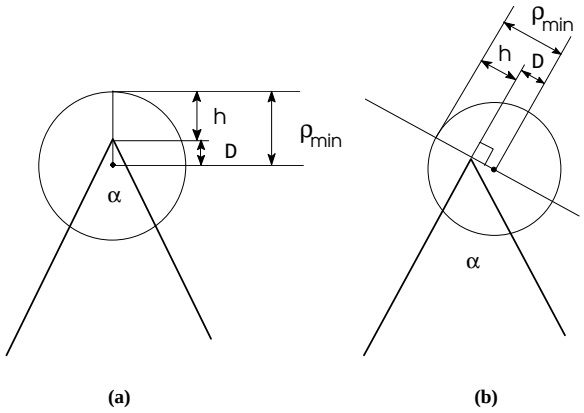

Figure 5: Modifications to the method to fix the deadlock in fig. 4

lem consists in replacing the circle drawn at each vertex with three circles of the same radius ρ_{min}. The center of the first circle lies on the bisector of the angle between the edges concurring in $\mathcal{X}_i$, at a distance $D = \rho_{min} - h$ from the vertex (see fig. 5–a). The centers of the second and third circles lie on the lines normal in $\mathcal{X}_i$ to the obstacle edges, at a distance $D = \rho_{min} - h$ (fig. 5–b). The rationale behind this heuristic is that the three circles approximate the envelope to the family of paths that "graze" the obstacle vertex. In fact, such envelope provides the shortest path on the extended visibility diagram (not necessarily the shortest bounded curvature path).

Remark 3. For a polygonal vehicle, the proposed algorithm and heuristics can be applied without major modifications obtaining qualitatively good results, as it has been verified in a number of simulations and experiments (see section 4). Consider for instance the simple planning problem for a Labmate in the environment depicted in fig. 6. The EPD obtained assuming $\rho_{min} = h$ is reported in fig. 6–a. Note that, due to the axial simmetry of the Labmate, all segments in EPD can be followed either way. In fig. 6–b the corresponding shortest path on the EPD is shown. Finally, fig. 6–c shows the path resulting from application of the heuristic discussed in remark 2 in the case that $\rho_{min} = 1.5h$. Note that, in spite of the considerable increase of the minimum turning radius, the path is still very close to the intuitive optimum. The described path planner can also provide a solution for car–like robots. The EPD of a parallel parking maneuver is reported in fig. 7–a (orientation of segments is not shown). The resulting maneuver looks quite natural, as shown in fig. 7–b. A more complex planning problem for a car–like vehicle is shown in fig. 8.

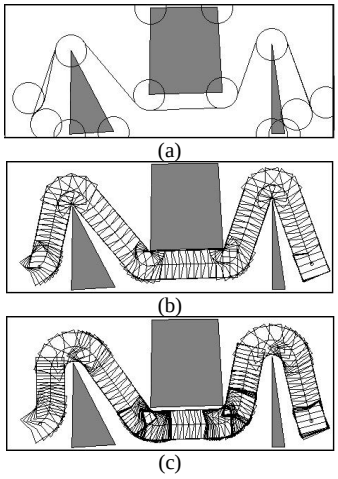

Figure 6: Planning the path of a Labmate with different turning radii. a) EPD for $\rho_{min} = h$; b) corresponding path; c) path corresponding to $\rho_{min} = 1.5h$.

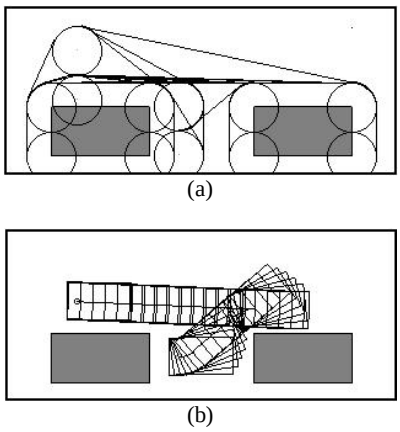

Figure 7: EPD (a) and final path (b) for the parallel–parking maneuver of a car–like vehicle.

4 Experimental

Experimental verification of the practical feasibility of the proposed planner has been carried out in our laboratory using a LABMATE robot of Transition Research, Inc.. The LABMATE kinematics are those of a unicycle, and its driving inputs are the torques applied to two independent wheels. The shape of the vehicle is loosely square, centered in the middle of the wheel axle. In order to accurately track planned trajectories, a Lyapunov–based closed loop control scheme has been employed, as described in [1]. The scheme

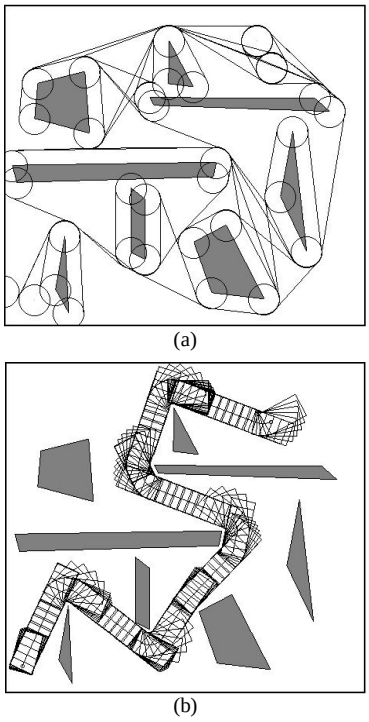

Figure 8: EPD (a) and resulting path (b) for a car–like vehicle in a cluttered environment.

showed good performance and robustness with respect to inaccuracies in the odometric measurement of positions caused by slippage at the wheels. The goal of our experiments was to verify the preliminar feasibility of an "automatic valet parking" of car–like vehicles in both a front and parallel parking lot. To this purpose, the shape of the LABMATE has been modified to resemble that of a car (in scale, approx. $80 \times 160cm$), and software has been written to implement a bound on the minimum turning radius of the vehicle (set to 40 cm). Detection of obstacles has been realized by using a set of US detectors available with the vehicle. US images are pre–processed and sent to the host computer (an Intel–486 based PC), via a radio serial link at 9600 baud. The host computer builds a simple 2D depth map of the scene and updates it while the vehicle moves down the parking lot corridor looking for a vacant slot. When room enough to maneuver the vehicle into is found, the planner process is started on the salient features of the map, and the resulting plan is executed directly after. In fig. 9 an experiment on parallel parking is described by the temporal sequence of phases. The updating of the experimental depth map superimposed to a picture of the actual environment

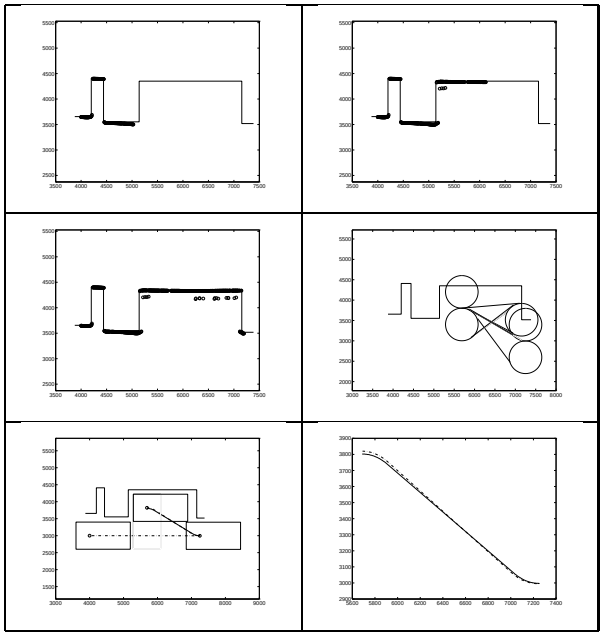

Figure 9: Sequence describing an experimental automated parallel parking maneuver. (a), (b), (c): US sensor signals are used to build a depth map of the parking lot as the vehicle scans the row; (d): Emended Path Diagram built by the planner; (e): parking maneuver; (f): planned path (solid) and actual trajectory (dashed).

configuration is shown in fig. 9 (a) through (c). It can be noted that sensor readings are rather accurate, except for a certain number of outliers, which have been taken care of by suitable processing. Fig. 9 (d) illustrates the construction of the EPD, while fig. 9 (e) shows the resulting parking maneuver. In fig. 9 (f) the traking error between the planned path and the trajectory actually followed by the Labmate is reported. The planning phase of such and similar experiments took less than 2 seconds, while the complete parking detection, planning, and execution took about 2 minutes. This was mainly due to the necessity of proceeding very slowly in the detection phase to avoid excessively large errors from the US sensors, and also slippage of wheels. The sensorial equipment of the vehicle resulted as one of the most critical components in the experiment. On the overall, the above reported experimental results confirmed the suitability of the proposed planner to real–time applications in near–future intelligent cars.

5 Conclusion

In this paper we have discussed a planning algorithm for nonholonomic, bounded curvature path

planning among obstacles whose output is the shortest feasible regular path for a particular vehicle. Although the proposed method is not complete, nor its optimality properties are trivially carried over to more general vehicles, very reasonable paths are generated by using only a few additional simple heuristics.

As compared with other methods known in the literature, the proposed planner does not need to build a supporting free path by means of configuration space methods nor does it require discretization of the configuration space. Paths generated by our method are typically very simple concatenations of Reeds/Shepp paths. An important quality of the proposed method is that it can be easily implemented even in cluttered workspaces, where the method actually performs comparatively best.

References

[1] M. Aicardi, G. Casalino, A. Balestrino, A. Bicchi: "Closed loop smooth steering of unicycle–like vehicles", Proc. 33rd Proc. Conf. on Decision and Control, pp. 2455–2458, 1994.

[2] J. Barraquand, J.C. Latombe: "Controllability of Mobile Robots with Kinematic Constraints", Technical Report No. STAN–CS–90–1317, Dept. of Computer Science, Stanford University, 1990.

[3] J.D. Boissonnat, A. Cerezo, and J. Leblond: "Shortest Paths of Bounded Curvature in the Plane", Proc. IEEE Int. Conf. on Robotics and Automation, pp.2315–2320, 1992.

[4] S.S.L. Chang: "Optimal Control in Bounded Phase Space", Automatica, vol. I, pp.55-67, 1963.

[5] G. Desaulniers: "On Shortest paths for a Car–like Robot Manouevering around obstacles"

[6] L. E. Dubins: "On curves of minimal length with a constraint on average curvature and with prescribed initial and terminal positions and tangents ", American Journal of Mathematics, vol.79, pp.497–516, 1957.

[7] P. Jacobs, J. Canny: "Planning Smooth Paths for Mobile Robots", *IEEE International Conference on Robotics and Automation*, AZ, 2–7, 1989.

[8] P. Jacobs, J. P. Laumond, M. Taix and R. Murray: "Fast and Exact Trajectory Planning for Mobile Robots and Other Systems with Nonholonomic Constraints", Technical Report 90318, LAAS/CNRS, Toulouse, France, September 1990.

[9] J. P. Laumond: "Feasible Trajectories for Mobile Robots with Kinematic and Environment Constraints", Proc. International Conference on Intelligent Autonomous Systems, Amsterdam, 346–354, 1986.

[10] J–C. Latombe: "Robot Motion Planning", Kluwer Academic Publishers, 1990.

[11] B. Mirtich, J. Canny: "Using Skeletons for Nonholonomic Path Planning among Obstacles", *IEEE International Conference on Robotics and Automation*, pp. 2533–2540, May 1990.

[12] J. A. Reeds, R. A. Shepp: "Optimal Paths for a Car that Goes both Forward and Backward", Pacific Journal of Mathematics, vol. 145(2), 1990.

[13] H. J. Sussmann and G. Tang: "Shortest Paths for the Reeds–Shepp Car: a Worked Out Example of the Use of Geometric Techniques in Nonlinear Optimal Control", SYCON report 91–10, 1991.